Influence of Injection Pressure on Ethanol and Gasoline Spray Penetrations in a Spark-Ignition Direct-Injection Fuelling System

Y. Bao[1], S. Padala[1], Q.N. Chan[1], S. Kook[1] and E.R. Hawkes[1, 2]

[1]School of Mechanical and Manufacturing Engineering
The University of New South Wales, Sydney, New South Wales 2052, Australia

[2]School of Photovoltaic and Renewable Energy Engineering
The University of New South Wales, Sydney, New South Wales 2052, Australia

Abstract

This study aims to assess the influence of injection pressure on ethanol and gasoline sprays in a spark-ignition direct-injection (SIDI) fuelling system. Specifically, the spray tip penetration of the ethanol and gasoline sprays at injection pressures of 4, 7, 11 and 15 MPa are measured from the Mie-scattered spray images collected in an optical spray chamber. From the measurements, the spray tip penetration is found to increase with increasing injection pressure for both ethanol and gasoline, which is to be expected. The penetration rates, however, are different for the ethanol and gasoline sprays. For example, the gasoline sprays show higher penetration rates at low injection pressures conditions. It is suggested that the higher viscosity of ethanol causes a greater frictional loss within the nozzle and thereby lower injection momentum flux. However, this friction loss becomes less significant when high injection pressure is applied. Therefore, the ethanol sprays are found to have higher penetration rates than the gasoline sprays at high injection pressure conditions. This trend is anticipated since the higher density, viscosity and surface tension as well as lower vapour pressure of ethanol would result in less breakup and evaporation.

Introduction

Spark-ignition direct-injection (SIDI) engines have several practical advantages over conventional port-fuel-injection (PFI) engines, such as better engine power and efficiency. This is because the direct injection of liquid fuel into the combustion chamber provides the opportunity for charge cooling, thereby increasing volumetric efficiency. The part-load efficiency is also higher due to reduced throttling, enabled by deliberate charge stratification to form a relatively richer mixture near the spark plug. Precise control of fuelling rate and reduced fuel injection duration associated with high injection pressure are the other advantages [3, 12]. While on-going research efforts are dedicated to achieve successful implementation of the SIDI fuel injection systems using conventional gasoline fuel, alternative biologically derived fuels are also being investigated due to the global concerns over the depletion of petroleum-based oils.

Ethanol has been widely accepted as one of the promising alternative fuels owing to its renewable nature as well as its anti-knock benefit. Ethanol-blend fuels are currently used in many countries. However, many details relating to sprays and mixture formation are still lacking for these ethanol-blend fuels and hence their potential impacts on the performances of SIDI engines are hard to assess. For instance, there are mixed results reported in the literature on the spray tip penetration of the ethanol spray in comparison with the gasoline spray. Gao *et al.* [4] and Wang *et al.* [10] have reported a higher spray penetration for gasoline than that of ethanol in their SIDI fuelling system. The reversed trend, however, has also been presented in the literature (*e.g.*, [5, 9]) whereby the ethanol spray is reported to penetrate further than gasoline at a fixed time after the start of injection. As such, there is no consensus for this simple question on the ethanol spray penetration.

To address this issue, we measured the ethanol and gasoline SIDI spray penetrations at fixed ambient temperature and pressure conditions. Of particular interest was the variation of penetration rates for the ethanol and gasoline sprays with injection pressure. Mie-scattering imaging was performed in an optical spray chamber to visualise the liquid phase sprays. The obtained images were post-processed to calculate and compare the spray penetration rates of the ethanol and gasoline sprays.

Experiments

Optical Spray Chamber

All injection events were conducted in an optically-accessible constant-volume chamber. Sight-glass windows are located in three sides of the chamber to provide optical access for side and bottom views of the sprays. A constant-flow compressed air at 0.1 MPa (gauge) was used to remove the fuel after each injection. The compressed air flow was necessary to maintain the same ambient air conditions as well as to prevent the liquid fuel droplets from contaminating the windows [8]. It is worth noting that the compressed air flow was sufficiently low so as to not affect the pressure drop across the nozzle. A schematic diagram of the optical spray chamber and Mie-scattering imaging setup is shown in figure 1.

The fuel supply system consists of a fuel tank, pump, rail and injector. The injector used in this work is a wall-guided 6-hole gasoline direct-injection injector (Continental DI XL2) used in a side-injection central-spark engine. The injector was positioned at the centre of the upper lid of the chamber. An injection duration of 0.5 ms was selected so that the injection ends before the spray tip goes out of the field of view. This approach allows visualisation of sprays not only during the injection but also a long time after the end of injection. Four injection pressures were tested, ranging from 4 MPa to the maximum injection pressure (15 MPa). The ambient temperature and pressure were fixed throughout the experiments. A summary of these operating conditions is listed in table 1.

Some properties of the fuels used in this study are presented in table 2. The table shows that compared with gasoline, ethanol has a lower vapour pressure and a higher density, viscosity, surface tension and heat of vaporisation. It also shows that gasoline is

associated with a range of boiling points, which is attributed to its multi-component nature. Some heavy components in the gasoline have higher boiling points than ethanol [1].

<u>Mie-Scattering Imaging Setup</u>

The setup of a strobe light and camera is illustrated in figure 1. A strobe light (Perkin Elmer X400) with 8~13 μs lighting duration was used to illuminate the liquid phase spray. An optical fibre cable was used to place the light source as close as possible to the chamber to allow optimum illumination of the liquid-phase fuel sprays. The scattered light from the sprays was captured by a CCD camera (Pike 421B), equipped with a 16-bit sensor. The pixel resolution of the image was about 16 μm. For the lens setup, an aperture opening of f/8 was selected to optimise brightness of the image and the depth of field. A camera exposure time of 70 μs was also specified to freeze the motion of the sprays.

With this camera setup, single-shot imaging was performed at several time intervals after the start of injection (aSOI). The image at the same time aSOI was repeated for 25 times to cycle-average the penetration data. The standard deviation (σ) of the measurements, derived from the 25 images (n = 25), was used to calculate the uncertainty range (e = $1.96\sigma/n^{0.5}$)[2]. The camera settings used are summarised in table 3.

<u>Image Processing</u>

All images collected were corrected for the background. Each corrected image was subsequently converted to a binary image using Otsu's boundary detection model — a widely used threshold-based method [6]. The spray tip penetration was then calculated from the spray boundaries.

Results and Discussion

Figure 2 shows a selected example of Mie-scattered ethanol spray images for various time intervals after the start of injection (aSOI). The injection pressure was set at 15 MPa. The images are presented in two rows: the first row shows the bottom-view images, and the second row is for the side-view images. The same imaging was repeated for injection pressures of 4, 7 and 11 MPa (not shown here) for both ethanol and gasoline sprays. On the left side of each spray image, the time stamps are given. The injector used in this study had 6 holes and the injection angle for each hole was different. Therefore, the spray tip penetration is derived from the distance from the tip of the central spray plume (plume C in figure 2) to the nozzle that appears to travel longest distance in the side-view image. The horizontal and vertical tip
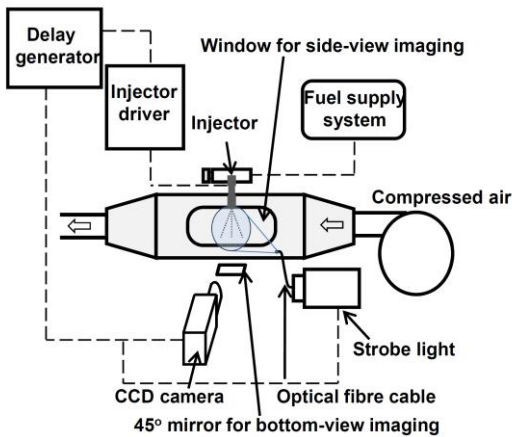

Figure 1 Schematic of spray chamber and Mie-scattering imaging setup.

Injector	Continental DI XL2
Number of holes	6
Injection duration (ms)	0.5
Injection pressure (MPa)	4, 7, 11, 15
Ambient temperature (K)	295
Chamber ambient pressure (MPa)	0.1 (gauge)

Table 1 Experimental conditions

	Ethanol	Gasoline
Density (kg/m^3)	794	720-780
Viscosity @ 20 ℃(Pa.s)	0.0012	0.00042
Vapour pressure @ 27 ℃ (MPa)	0.018	0.045-0.09
Surface tension (N/m)	0.023	0.019
Boiling point (℃)	78.5	30-200
Heat of vaporization (kJ/kg)	904	310

Table 2 Fuel properties of ethanol and gasoline

CCD camera	Pike 421B
Image resolution	0.016 mm
Exposure time	70 μs
Lens	50 mm, f/8

Table 3 Camera settings.

penetrations of this central plume were obtained from the bottom-view and side-view images, respectively, as shown in figure 2. The tip penetration along the axis of the spray was subsequently derived from these distances using trigonometric function. Figure 2 shows a rapid penetration of multiple spray plumes until the end of injection. Later, the spray tip penetration decelerates as the axial injection momentum diminishes. Disappearance of bright signals around the boundaries of sprays at later timings is a clear indication that the spray has collapsed slightly and evaporation has occurred.

The penetration trend seen in figure 2 is well reflected in the spray tip penetration plot in figure 3. The tip penetration was normalised by the maximum tip penetration measured at 1.2 ms aSOI for the selected condition. It is noted the overlapping of adjacent spray plumes prevented the accurate determination of the central plume penetration at the start of injection. Hence, the data are only presented after 0.4 ms aSOI. Moreover, the end-of-injection occurs at 0.5 ms aSOI when 43% penetration is achieved. It should be noted that the spray imaging was repeated for 25 times, and the error bars associated with the statistical uncertainty for each data point are presented in figure 3. The uncertainty is found to be very small such that the depicted error bars are smaller than the marker diameter for the data in figure 3.

As mentioned previously, the same spray imaging and data analysis procedure were repeated for all of the investigated injection pressures, and for both ethanol and gasoline. From these data, the spray tip penetration rates for various injection pressures were determined as shown in figure 4. The figure shows four different viewgraphs drawn for various penetration stages (*i.e.*
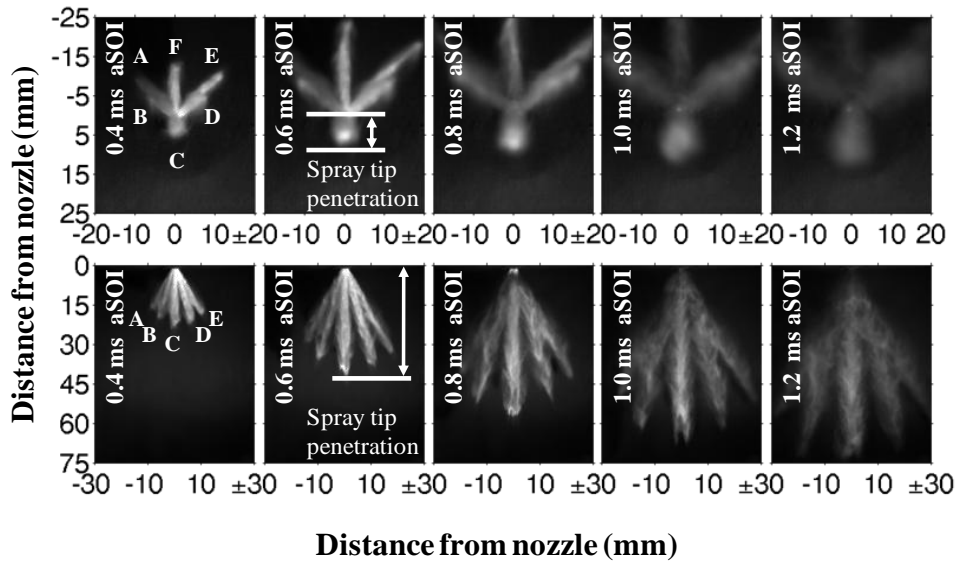
Figure 2 Bottom-view (top) and side-view (bottom) images of ethanol sprays for various time after the start of injection (aSOI). The pressure drop across the nozzle (*i.e.* injection pressure) is 15 MPa.

percentage of the maximum penetration). Also shown for the 45~85% penetration plots are the inset plots of the spray tip penetration rate of the PFI that are reproduced from ref. [8]. These data are complementary to the SIDI sprays injected at 4~15 MPa as the injection pressure of the PFI system was set at much lower 0.25 MPa, with an injection duration of 3 ms. The ambient air pressure and temperature of the PFI case were also fixed at 0.1 MPa and 295 K, respectively.

The first noticeable trend from figure 4 is that at 35% and 45% penetration stages, the gasoline spray shows a higher tip penetration rate than that of the ethanol when low injection pressures of 4 MPa was used. This was consistent with the PFI results obtained at much lower injection pressure. The higher penetration rates of gasoline were not anticipated because lower density, viscosity and surface tension as well as higher vapour pressure (see table 2) would lead to higher breakup and evaporation of sprays. As mentioned previously, cycle-to-cycle fluctuations are insignificant and therefore the measured variations are well outside of the uncertainty.

It is obvious that the influence of the fuel property on the spray dynamics alone cannot explain the observed trend. Therefore the fuel injection condition should be considered. For instance, whilst the higher viscosity of ethanol might suppress breakup and evaporation, a higher friction loss within the injector nozzle would result in a lower injection momentum flux [11] and hence a decrease in the penetration rate. Another common theory to explain the higher penetration rate of the gasoline spray than the ethanol is the multi-component nature of a conventional gasoline [4, 5, 7, 10]. In other words, the heavy components (heavier than ethanol) of gasoline might experience breakup and evaporate processes at a slower rate than ethanol. It is not possible, however, with the present information to assess the significance of this effect.

The influence of the friction loss and heavy components in gasoline appears to be less significant when higher injection pressures are used. Figure 4 shows that the increase of the spray tip penetration rate with increasing injection pressure is more significant for ethanol than that of gasoline. For example, the tip penetration rate is higher for ethanol at the injection pressure of 15 MPa regardless of the penetration stages. Another interesting
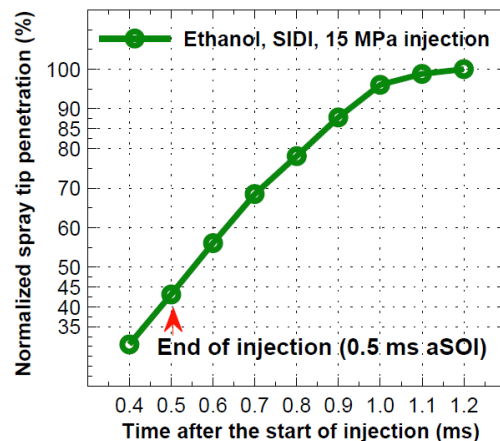

Figure 3 Ethanol spray tip penetration at 15 MPa injection pressure.

finding from figure 4 is that the deceleration of the penetration after the end of injection (*i.e.* 45~85% penetration) is higher for gasoline causing higher ethanol spray penetration even at low injection pressure ranges (except the PFI case). The same trend was found in ref. [1] where higher plume velocity was measured for gasoline during the injection; however, after the end of injection the trend was reversed such that the plume velocity was higher for ethanol. Therefore the result suggests that less breakup and evaporation associated with the fuel property becomes evident only if the injection pressure is high enough to overcome the frictional loss and when the spray penetration decelerates significantly as the axial injection momentum diminishes.

Conclusions

Mie-scattering imaging has been performed in an optical spray chamber to investigate the effect of injection pressure on the ethanol and gasoline spray penetrations in a spark-ignition direct-injection (SIDI) fuelling system. The spray tip penetrations were derived from the vertical and horizontal spray penetration distances measured from the side-view and bottom-view images, respectively. The findings of this study are as follows:
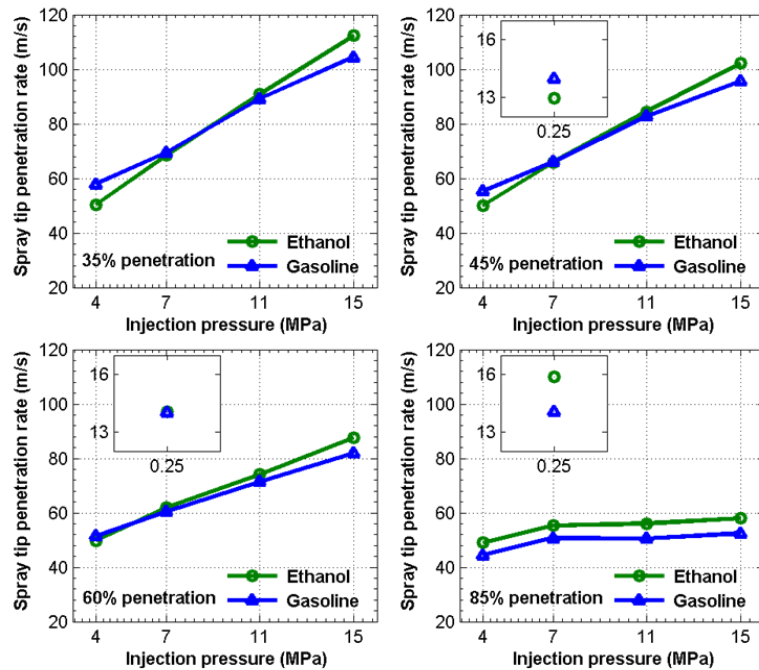
Figure 4 Spray tip penetration rate for various injection pressures at 35, 45, 60 and 85% of the maximum penetration distance. Shown at the top-left of each of 45~85% penetration figures is the penetration rate for a port fuel injector from ref. [8].

1. The tip penetration rates of the gasoline sprays are found to be higher than that of the ethanol sprays when the injection pressure is low. This is likely attributed to the higher viscosity of ethanol and hence greater frictional loss within the nozzle.

2. The physical property of ethanol such as higher density, viscosity and surface tension, in addition to lower vapour pressure would cause higher tip penetration than that of gasoline due to lower breakup and evaporation. This is evident when the influence of the friction loss becomes less significant as high injection pressure is applied.

3. The increase of the spray tip penetration rate with increasing injection pressure is more significant for ethanol than that of gasoline. Also, the deceleration of the tip penetration after the end of injection is higher for gasoline. As a result, the spray tip penetration is high for the ethanol sprays for all injection pressures studied for the SIDI system long time after the engine of injection when the axial injection momentum becomes very low.

Acknowledgments

References

[1] Aleiferis, P.G. & van Romunde, Z.R., An Analysis of Spray Development with Iso-octane N-pentane Gasoline Ethanol and N-butane from a Multi-Hole Injector under Hot Fuel Condition, *Fuel*, 2012, DOI: 10.1016/j.fuel.2012.07.044.

[2] Antonius, R., *Interpreting Quantitative Data with SPSS*, London, Sage Publications Ltd., 165-467, 2004.

[3] Drake, M.C. & Haworth, D.C., Advanced Gasoline Engine Development using Optical Diagnostics and Numerical Modelling, *Proc. Combust. Inst.,* **31**, 2007, 99-124.

[4] Gao, J., Jiang, D. & Huang, Z.H., Spray Properties of Alternative Fuels: A Comparative Analysis of Ethanol-Gasoline Blends and Gasoline, *Fuel*, **86**, 2007, 1645-1650.

[5] Matsumoto, A., Moore, W.R., Lai, M.C., Zheng, Y., Foster, M., Xie, X.B., Yen, D., Confer, K. & Hopkins, E., Spray Characterization of Ethanol Gasoline Blends and Comparison to a CFD Model for a Gasoline Direct Injector, *SAE Int. J. Engines*, **3**, 2010, 402-425.

[6] Otsu, N., A Threshold Selection Method from Gray-Level Histograms, *IEEE T. Syst. Man. Cyb.*, **9**, 1979, 62-66.

[7] Park, S.H., Kim, H.G., Suh, H.K., & Lee, C.S., Atomization and Spray Characteristics of Bioethanol Blended Gasoline Fuel Injected through a Direct Injection Gasoline Injector, *Int. J. Heat Fluid Fl.,* **30**, 2009, 1183-1192.

[8] Padala, S., Kook, S. & Hawkes, E., Effect of Ethanol and Ambient Pressure on Port-Fuel-Injection Sprays in an Optically Accessible Intake Chamber, *Atomization Spray,* **21**, 2011, 427-445.

[9] Sementa, P., Vaglieco, B.M. & Catapano, F., Influence of the Injection Pressure on the Combustion Performance and Emissions of Small GDI Engine Fuelled with Bio-ethanol, *SAE Tech. Pap. Ser.* 2011-37-0007, 2011.

[10] Wang, X.B., Gao, J., Characteristics of High-Pressure Swirl Injector Fueled with Methanol and Ethanol**,** *Energy Fuels*, **19**, 2005, 2394-2401.

[11] Zeng, W., Xu, M., Zhang, M., Zhang, Y. & Cleary, D.J., Macroscopic Characteristics for Direct-Injection Multi-Hole Sprays Using Dimensionless Analysis, *Exp. Therm Fluid Sci.,* **40**, 2012, 81-92.

[12] Zhao, F., Lai, M.C. & Harrington, D.L., Automotive Spark-Ignited Direct-Injection Gasoline Engines, *Prog. Energy Combust. Sci.,* **25**, 1999, 437-562.